



Research article

Retrofit and application of pulverized coal burners with LNG and oxygen ignition in utility boiler under ultra-low load operation

Hujun Zhao ^a, Weiqi Li ^{b,*}, Jie Zhang ^c, Xian Ding ^d, Zhizhong Kang ^c^a CHN Energy Long Yuan Blue Sky Energy Conservation Technology Co., Ltd., Beijing 100039, China^b GD Power Development Co., Ltd., Beijing 100101, China^c School of Energy Power and Mechanical Engineering, North China Electric Power University, Beijing 102206, China^d Shanghai Power Equipment Research Institute Co., Ltd., Shanghai 200240, China

ARTICLE INFO

Keywords:

Boiler retrofit
Burner
LNG
Deep peak shaving
NOx emissions
Combustion
Numerical simulation

ABSTRACT

An oxygen-rich and low NO_x burner integrated with liquefied natural gas (LNG) was proposed to address unstable combustion and high NO_x emissions from a 330 MW subcritical boiler under ultra-low load operation in China. To assess the effectiveness of the retrofit, Chemkin and Fluent softwares were utilized to construct a new NO_x model and calculate NO_x generation, based on the combustion of pulverized coal gas and LNG. Further, an eddy dissipation concept (EDC) model, which can reflect detailed chemical reactions, was applied to calculate gas-phase reactions in the furnace. The results showed that when performing the deep peak shaving after the retrofit, the combustion in the furnace was stable under 50% or more load, and NO_x emission level at the furnace outlet was lower than 350 mg/m³ (6% O₂ content, dry basis). Under 25% load, the oxygen-rich burner integrated with LNG was applied, and the pulverized coal flow entered the furnace in a state of high-intensity combustion, which effectively promoted the stability of combustion in the furnace. The reductive combustion state with reductive free radicals generated by LNG decomposition inhibited NO_x formation. Consequently, NO_x emissions from the furnace outlet decreased from 380 mg/m³ to 316 mg/m³.

1. Introduction

Thermal power technology in China is constantly evolving. Currently, 300 MW thermal power generating units, especially units using lean coal, are facing tough competition and peak regulation [1–3]. Although several coal-fired generating units with larger capacity and higher efficiency parameters have been built, some 300 MW units are striving to meet flexible transformation requirements and achieve stable combustion under low load and low pollutant discharge to ensure economic viability [4–7].

Several local and global studies have conducted experiments and numerical calculations to address problems faced by coal-fired boilers operating under low load. Research has indicated that the steady combustion effect can be improved moderately by reducing pulverized coal fineness, controlling the oxygen content in the furnace, and reasonably laying the protective combustion zone [8,9]. When the boiler is operated at 500–800 MW load, the furnace temperature is relatively high, and a large excess air coefficient is adopted to help the coal powder burn out. However, when the peak load is as low as 300 MW, the oxygen at the outlet of the furnace must be controlled at approximately 3% to improve the combustion temperature in the furnace and achieve stable combustion.

* Corresponding author.

E-mail address: LiWeiQi_GDDL@163.com (W. Li).

<https://doi.org/10.1016/j.heliyon.2024.e29154>

Received 5 January 2024; Received in revised form 16 March 2024; Accepted 2 April 2024

Available online 8 April 2024

2405-8440/© 2024 The Author(s). Published by Elsevier Ltd. This is an open access article under the CC BY-NC-ND license (<http://creativecommons.org/licenses/by-nc-nd/4.0/>).

Tsumura et al. [10] conducted a single burner combustion test on a new burner with a flame stabilization ring and special air nozzle and achieved 50% minimum stable operating load of the burner (boiler operating load of 30–40%) and nitrogen oxide emissions below 200 mg/m³ (6% O₂ content, dry basis). A field test conducted by Yang et al. [7] on a 330 MW lean coal boiler revealed that the NO_x concentration in the inlet section of selective catalytic reduction (SCR) was relatively stable (< 600 mg/m³) when the boiler was operated under a stable load; however, NO_x concentration in the inlet section of the SCR was high (> 650 mg/m³) when the boiler was operated under variable load and low load.

Domestic and foreign studies on low NO_x and deep peak regulation suggest that solutions for the low NO_x transformation of coal-fired boilers available currently are relatively mature [11,12]. However, stable combustion and pollutant emission control, which comply with national environmental protection standards under deep peak regulation, have to be identified urgently [13,14]. Currently, thermal power units in China are facing multiple obstacles such as poor coal quality, coal consumption reduction, peak depth adjustment, and ultra-low pollutant discharge standards. In this light, China Guodian Corporation conducted a research on unit number 2 of their Shizuishan power plant, and proposed a set of transformation plans constituting oxygen-rich and low NO_x burners integrated with LNG to resolve the problems currently faced by 330 MW boilers.

The study used Chemkin software to calculate the NO_x generation and reduction process of LNG-mixed coal gas flow during combustion to explore the reaction mechanism and verify the feasibility of the scheme. Additionally, the reactions were selected and simplified based on the combustion of various components and feasibility of Fluent simulation, and a new gas-solid mixed NO_x model was constructed. Then, an eddy dissipation concept (EDC) was employed to calculate the gas reaction in the furnace. The NO_x model constructed was applied to Fluent software to simulate the combustion performance and NO_x generation under deep peak regulation of the boiler after the retrofit. Furthermore, field test data and simulation results were used for comparative analysis.

2. Methodology

NO_x includes a variety of nitrogen oxides and their generation mechanism is complicated and not fully understood [15–17]. Low load stable combustion is based on reducing the ignition heat of pulverized coal by increasing the primary air temperature and concentration of pulverized coal, and reducing the primary air rate and fineness of pulverized coal [18–20]. Therefore, this study constructed a new NO_x model and performed numerical calculations based on the retrofit scheme of integrated LNG, oxygen enriched, and low NO_x burners proposed by China Guodian Corporation.

2.1. Proposed retrofit scheme

Three major measures were implemented in the retrofit to achieve deep peak shaving while ensuring stable combustion and reduction in NO_x production. These are summarized in Fig. 1(a) to Fig. 1(c).

(a) Adjustment to the main burner layout: Before this low-nitrogen and peak-shaving transformation, the power plant had undergone a previous transformation, shifting the burner arrangement from front-wall placement (four layers) to front-and-rear wall placement (three in front, one in rear), resulting in the mismatch of the main aerodynamic field in the furnace with the original design. The main burner at the bottom of the rear wall was eliminated (Fig. 1(a)) and the main burner on the fourth floor was arranged on the front wall (Fig. 1(c)).

(b) Addition of oxygen enriched and low NO_x burners: The original swirl burner structure includes primary air carrying coal powder, rotating internal secondary air and external secondary air, and a small amount of center air. The primary air passage of the burner is equipped with a swirl device, and the primary air flow rate is relatively high, while the internal and external secondary air flow rates are relatively low, causing the coal powder to be injected into the furnace in a rotating state with the primary air. Some of the coal powder prematurely diffuses radially due to centrifugal force, leading to premature ignition and an oxygen-rich combustion environment, generating a large amount of NO_x. Additionally, it increases the ignition temperature of the coal powder airflow, resulting in poor combustion stability at low loads [21,22]. Fig. 1(b) illustrates the design of oxygen-rich, low NO_x burner integrated with LNG. The second-tier burner of the boiler was transformed into a new burner, and an oxygen supply system, gas system, and control system were installed. (c) Adjustment of layout plan for over-fired air and near-wall air: The original location of the over-fire air is unreasonable, with the over-fire air placed at a height of 30.5 meters above the water-cooled wall and 7.1 meters away from the top-level main burner. After the transformation, the position of the over-fire air needs to be raised to increase the combustion space of coal powder. The original furnace did not have near-wall air, and the high sulfur content of the coal entering the furnace led to the generation of a large amount of H₂S in the water-cooled wall area during adjustments for air-staged combustion, causing high-temperature corrosion [23]. The original over-fired air nozzles were eliminated and twelve over-fire air nozzles (six each on the front wall and rear wall) were rearranged 1.1 m above the original over-fire position. In the area above the three main burners on the front wall (near the water wall of the side wall), three near-wall air nozzles were added respectively. Further, two near-wall air nozzles were installed on the top layer of the rear wall corresponding to the front wall. The specific placements are depicted in Fig. 1(a) and Fig. 1(c).

The goal of retrofit scheme proposed to operate six oxygen enriched and low NO_x burners on the second layer when the boiler was undergoing deep peak shaving, with a minimum of 20% of the rated load for ultra-low load peak shaving. When oxygen enriched combustion technology is used, the modified design coal for combustion can reach the peak shaving range of 20–100% of the rated load without affecting the relevant parameters of the boiler under the original operating conditions. After operating the oxygen enriched and low NO_x burners, the hourly average concentration of NO_x emission from the furnace outlet of the unit is not higher than 350 mg/Nm³ (6% O content, dry basis).

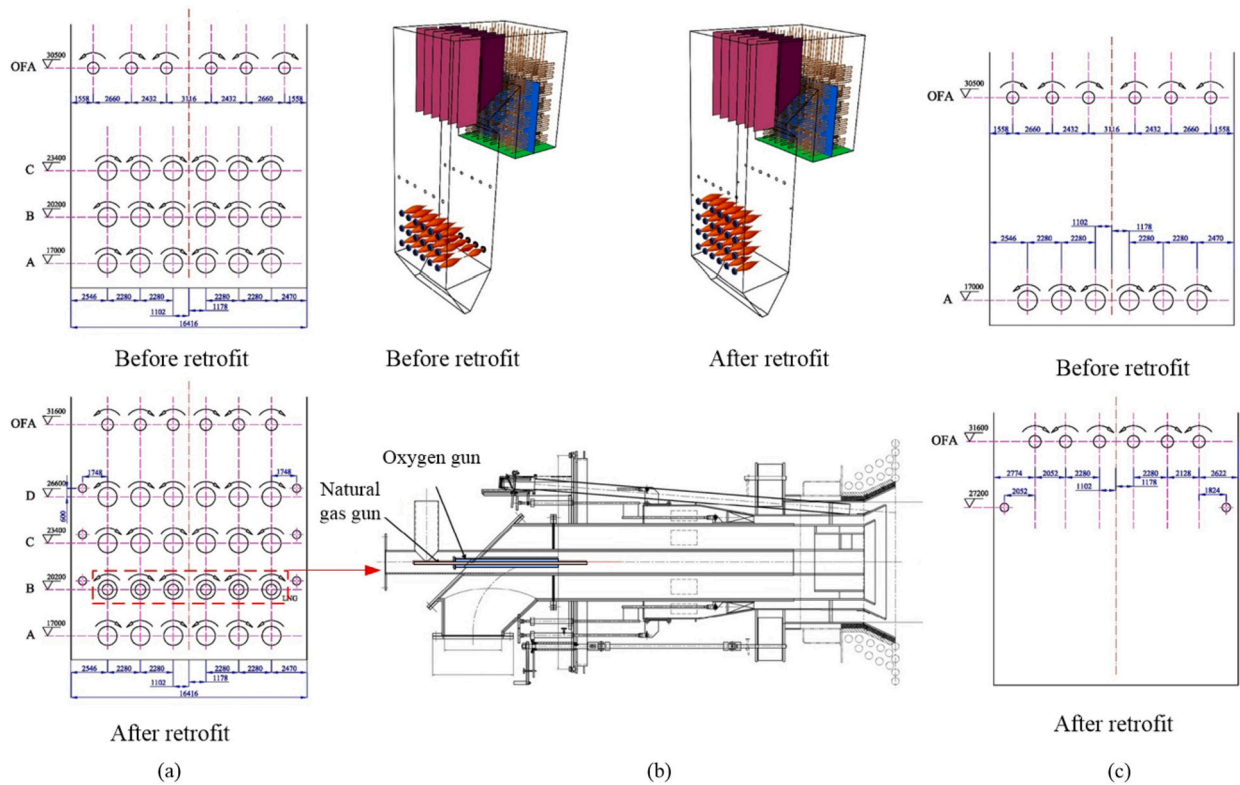


Fig. 1. 330 MW face-fired boiler retrofit scheme.

Table 1
Design coal quality after transformation.

Industrial analysis (wt%, ar)	Fixed carbon	37.51
	Volatile	18.13
	Ash	37.06
	Moisture	7.3
Elemental analysis (wt%, daf)	C	79.58
	H	4.98
	O	10.82
	N	1.64
	S	2.98
LHVar (kJ/kg)	–	16820

ar: As received basis; daf: Dry ash-free basis; LHV: Low heating value.

2.2. Construction of NO_x model

2.2.1. Simulated reactor model

Chemkin was used to calculate the process of NO_x generation and reduction, based on the combustion characteristics of pulverized coal with LNG. A plug flow reactor was used in Chemkin to simulate the chemical reaction in a one-dimensional flow system. In the solution process, only the mass, momentum, gas composition, and state governing equations were calculated, and the energy equation was not solved. The model assumed that the temperature was constant during the reaction and was set on the basis of multiple conditions of pulverized coal combustion. Table 1 lists the coal type data of the proposed design.

The methods to simplify the volatile combustibles proposed in the literature were adopted in this study [24,25]. Further, CH₄, CO, and H₂ were assumed to be the combustible substances in the volatile matter. The study assumed that H and O in the pulverized coal were separated out, N elements were separated out as HCN, and S elements were separated out as S. The corresponding coke component was simplified to CO₂ and CO according to different excess air coefficients in the simulation conditions. Further, based on the conservation of the mass of each element, energy conservation between the assumed components after complete combustion and the low calorific value of the coal, iterative verification was performed until the two conservation errors were controlled within 5%. Table 2 lists the mass ratio of each component, assuming that the pulverized coal was gas under various excess air coefficients.

Table 2
Hypothetical composition and mass ratio of pulverized coal pyrolysis.

α	CH ₄	CO	H ₂	HCN	S	H ₂ O	CO ₂	O ₂	N ₂
0.8	0.64	4.75	0.34	0.33	0.31	1.36	20.49	5.17	66.61
0.9	0.57	2.81	0.31	0.29	0.28	1.22	21.84	5.23	67.45
1.0	0.53	1.24	0.29	0.27	0.26	1.13	21.37	5.39	69.52
1.1	0.49	1.14	0.26	0.25	0.24	1.04	19.60	6.87	70.11
1.15	0.47	1.09	0.25	0.24	0.23	1.00	18.82	7.52	70.38

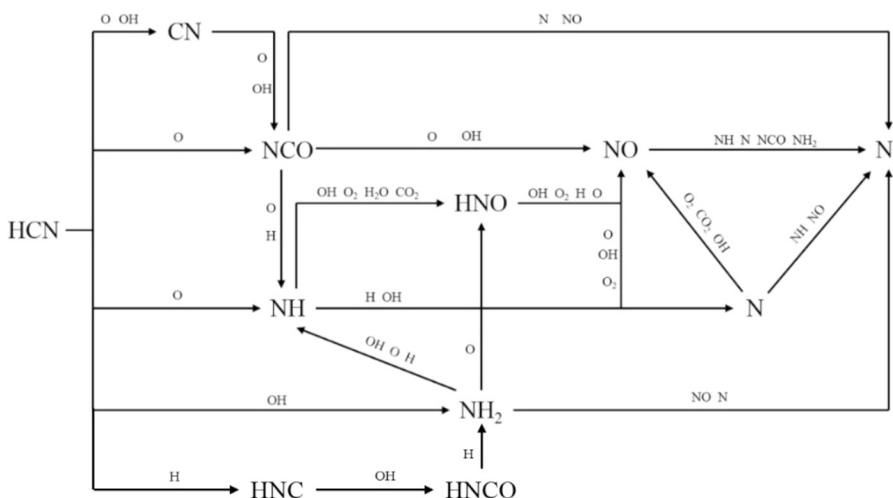


Fig. 2. Reaction pathway of HCN after optimization.

Table 3
Main reactions involved in HCN oxidation to NO.

No.	Reaction	No.	Reaction
1	HCN + O ⇌ NCO + H	15	NH + H ⇌ N + H ₂
2	HCN + OH ⇌ CN + CO	16	NH + O ⇌ N + OH
3	HCN + H ⇌ HNC + H	17	HNCO + H ⇌ CO + NH ₂
4	HCN + O ⇌ NH + CO	18	N + O ₂ ⇌ NO + O
5	HCN + O ⇌ CN + OH	19	N + CO ₂ ⇌ NO + CO
6	HCN + OH ⇌ NH ₂ + CO	20	N + OH ⇌ NO + H
7	H + NCO ⇌ NH + CO	21	N + NO ⇌ O + N ₂
8	CN + O ₂ ⇌ NCO + O	22	NH ₂ + NO ⇌ N ₂ + H ₂ O
9	HNC + OH ⇌ HNCO + H	23	NH ₂ + N ⇌ N ₂ + H + H
10	NH + O ⇌ NO + H	24	HNO + O ⇌ NO + OH
11	NH + SO ⇌ NO + SH	25	HNO + H ⇌ NO + H ₂
12	NH + O ₂ ⇌ HNO + O	26	HNO + M ⇌ NO + H + M
13	NH + OH ⇌ HNO + H	27	HNO + OH ⇌ NO + H ₂ O
14	NH + CO ₂ ⇌ HNO + CO	28	HNO + O ₂ ⇌ NO + HO ₂

2.2.2. Simplification of the reaction mechanism

This study assumed that all nitrogen-containing substances in the pulverized coal were released in the form of HCN, which was precipitated into the flue gas during the flow and heating of pulverized coal. Subsequently, HCN was subject to complex and diverse chemical reactions. ROP analysis and sensitivity analysis indicate that the oxidation process of HCN was optimized. The optimized reaction pathway of HCN is illustrated in Fig. 2.

Following volatilization, HCN was mainly converted into nitrogenous substances such as NCO, CN, HNC, NH, and NH₂ through elementary reactions. Chemkin was used to analyze the mechanism of HCN oxidation to NO. After eliminating smaller proportions of the reaction path, a backbone reaction consisting of 28 steps was constructed, as listed in Table 3.

Further, the main component of LNG is CH₄. CH₄ undergoes a series of complex reactions with O₂ under high temperature and high oxygen concentration to finally generate CO₂ and H₂O. In a reducing atmosphere, the reaction rate is relatively low. CH₄ initially decomposes to form a hydrocarbon group CH₁, and subsequently the hydrocarbon group reduces nitrogen oxides to an intermediate product, HCN. In the current scenario, the CH₄ in LNG reduced NO during the combustion process, as listed through the reactions below.

CH₄ was firstly decomposed to CH₃ during the combustion process:



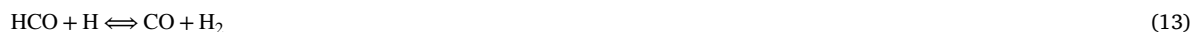
CH₃ reduced NO, and reacted further to form CH₂, and some CH₂O:



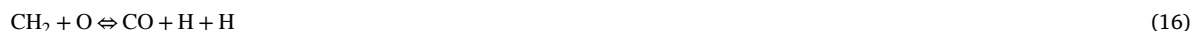
The generated CH₂O was converted to HCO through the following path:



HCO was converted to CO and H₂ through the following reaction:



However, CH₂ is highly active and can react with many substances, resulting in the production of CH and reduction of NO:



The generated CH could also reduce NO and react with other substances:



The oxidation process of HCN and reduction of NO by LNG were incorporated in the NO_x model used in the computational fluid dynamics (CFD) calculation.

2.3. Numeral calculations

2.3.1. Face-fired boiler

The 330 MW subcritical pressure, face-fired boiler used in this study was designed and configured to burn bituminous coal. The relevant design parameters of the boiler following the retrofit are listed in Table 4. The simulation process considers the panel superheater at the top of the furnace and part of the convective heating surface at the exit of the furnace. The heat transfer tube was simplified to a flat plate and a porous medium to simplify the model.

In the simulation, 139.51 t/h of coal was introduced into the furnace under BMCR load to produce 1004 t/h of superheated steam at a pressure of 18.50 MPa and temperature of 543 °C. To completely consume the fuel, 1147.86 t/h of combustion air had to be supplied. In the simulation process, the fuel composition and coal properties were considered to be identical to the coal quality used

Table 4
Relevant design parameters of the boiler after transformation.

Project	Unit	Value
Furnace (width × depth × height)	mm ³	16416 × 11096 × 51300
Horizontal distance of the burner	mm	2280
Vertical distance of the burner	mm	3200
Distance between the uppermost burners and bottom of the panel superheater	mm	16100
Distance between the uppermost burners and OFA	mm	5000

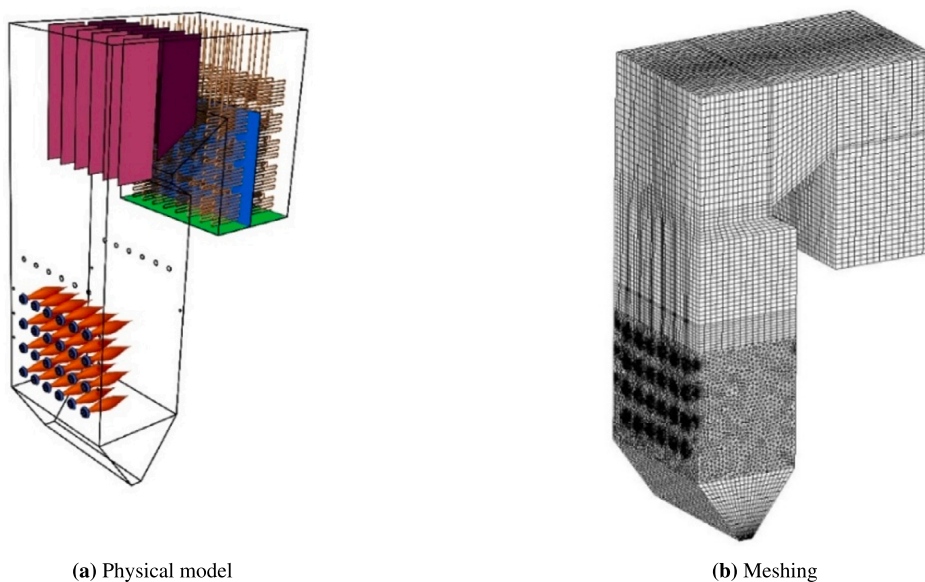


Fig. 3. Physical model and meshing of furnace number 2 after retrofit.

in the power plant boiler. Results of the industrial analysis and elemental analysis of the designed coal type after transformation are listed in Table 1.

2.3.2. Numerical simulation of pulverized coal combustion in boiler under different loads

Fluent was used to simulate the combustion of pulverized coal in the boiler under full scale and four loads. Additionally, the EDC model was utilized to examine the mechanism of the reaction process, and particle surface combustion reaction was used to consider the process of heterogeneous reduction of NO_x.

The simulation area included areas from the cold ash hopper to the economizer outlet section. A physical model based on the actual boiler size was established in the proportion of 1:1. A schematic diagram of the furnace structure after the retrofit is shown in Fig. 3(a). The inlet of the swirl burner was simplified to a concentric circle structure. The panel superheater at the top of the furnace was simplified to a flat plate. The simplified area was consistent with the actual heat exchange area. ICEM was used to mesh the physical model. Unstructured grids divided the main combustion zone. The grid was encrypted near the burner exit, and structural grids divided other areas. The grid division of the furnace after the transformation is depicted in Fig. 3(b).

During the meshing process, the independence of the computational results on the number of grid cells is verified by comparing the results under different grid sizes and numbers. Models with grid numbers of 954,265, 1153,658, and 1352,334 are selected, and the same boundary conditions are set to obtain the average temperature and its variation on the furnace cross-section. Although there are some differences in the calculated results under different grids, the overall trend is consistent, and the differences are small. The fitting results are good. Therefore, considering the computational capabilities and the accuracy of the results, the final decision is to use approximately 1150,000 grid cells for the entire domain.

This study used three boundary conditions: velocity inlet, pressure outlet, and wall condition. The velocity inlet boundary condition pertained to the air supply, which was sent into the furnace through the primary air nozzle, secondary air nozzle, over-fire air (OFA) nozzle, and near-wall air nozzle. A pressure outlet boundary condition was applied at the outlet of the simulation area, applying a slight negative pressure of 50 Pa and backflow temperature of 1000 K. The discrete phase boundary condition type at the exit of the furnace was set to “Escape”, when coal particles left the furnace at the exit. The wall boundary conditions assumed that the temperature of all heated surfaces (including water walls and superheaters) was constant and the temperature was 50 °C higher than the temperature of the working fluid at the corresponding location. The convective heating surface of the tail was set with porous media [26]. Different constant heat losses under different working conditions were set to simulate heat absorption of the heating surface. The main boundary conditions of boiler operation under a BMCR load were set as shown in Table 5.

Table 5
Settings of the simulation working condition.

Air mass flow (kg/s)	Primary air	51.040
	Internal secondary air	25.520
Temperature of air entering the furnace (°C)	External secondary air	93.574
	Over fire air	60.047
	Primary air	75
Coal consumption (kg/s)	secondary air	305
	–	38.64
Excess air coefficient of main combustion zone	–	0.85
Overall excess air coefficient	–	1.15

The continuous phase of flue gas was modeled using the Reynolds average Navier-Stokes equation, and the Realizable $k-\epsilon$ two-equation gas turbulence model was selected and combined with the standard wall function to model the wall [27]. The governing equation can be expressed as:

$$\frac{\partial(\rho u\varphi)}{\partial x} + \frac{\partial(\rho v\varphi)}{\partial y} + \frac{\partial(\rho w\varphi)}{\partial z} = \frac{\partial}{\partial x} \left(\Gamma \frac{\partial\varphi}{\partial x} \right) + \frac{\partial}{\partial y} \left(\Gamma \frac{\partial\varphi}{\partial y} \right) + \frac{\partial}{\partial z} \left(\Gamma \frac{\partial\varphi}{\partial z} \right) + S \quad (25)$$

where, ρ represents the continuous phase density (kg/m^3), φ represents the general physical variables, Γ represents the universal coefficient, and S represents the source term.

The discrete phase model was used to simulate the particle phase [28]. The particle trajectory was calculated using Eq. (26).

$$\frac{d\vec{u}_p}{dt} = \frac{18}{\rho_p d_p^2} \frac{C_D Re}{24} (\vec{u} - \vec{u}_p) + \frac{g(\rho_p - \rho)}{\rho_p} \quad (26)$$

where, \vec{u}_p represents the velocity vector of particle motion (m/s), \vec{u} represents the velocity vector of the continuous phase motion (m/s), ρ_p represents the grain density (kg/m^3), C_D represents the coefficient of particle resistance under turbulence pulsation, d_p represents the grain diameter (m), and Re represents the Reynolds number.

When the particles attained the set volatile release temperature after heating, the simulation was set to 500 °C, and volatiles were precipitated using the dual competitive release model [29]. The governing equations are expressed in Eqs. (27)- (29). The volatile components are expressed in Eq. (30).

$$\frac{m_v(t)}{(1 - f_{w,0}) m_{p,0} - m_a} = \int_0^t (\alpha_1 R_1 + \alpha_2 R_2) \exp \left(- \int_0^t (R_1 + R_2) dt \right) dt \quad (27)$$

$$R_1 = A_1 \exp \left[- (E_1 / RT_p) \right] \quad (28)$$

$$R_2 = A_2 \exp \left[- (E_2 / RT_p) \right] \quad (29)$$

$$\begin{aligned} \text{Volatile} = & 0.21345\text{CH}_4 + 0.2857\text{CO} + 0.9256\text{H}_2 \\ & + 0.0405\text{H}_2\text{O} + 0.05187\text{S} + 0.065\text{HCN} \end{aligned} \quad (30)$$

where, $f_{w,0}$ represents the initial moisture ratio in the particle; T_p represents the particle temperature (K); R_1 and R_2 respectively represent rate of primary and secondary reactions (s^{-1}); m_a represents the ash mass in particles (kg); $m_{p,0}$ represents the initial particle mass (kg); A_1 is the pre-exponential factor of the primary reaction, $2.0 \times 10^5 \text{ s}^{-1}$; A_2 is the pre-exponential factor of secondary reaction, $1.3 \times 10^7 \text{ s}^{-1}$; E_1 is the activation energy of primary reaction, $1.04 \times 10^8 \text{ J/mol}$; and, E_2 is the activation energy for the secondary reaction, $1.67 \times 10^8 \text{ J/mol}$.

P-1 radiation model was used to simulate radiation heat transfer during the simulation of the combustion process [30]. The radiant heat flow was calculated using Eq. (31) [31].

$$q_r = - \frac{1}{3(a + \sigma_s) - C\sigma_s} \nabla G \quad (31)$$

where, a represents the Absorption coefficient; σ_s represents the Scattering coefficient; and G represents the incoming radiation.

The convective heat transfer area at the tail was set as a porous medium area and was processed by adding momentum loss (internal loss and viscous loss) to the continuous phase momentum equation. The added momentum source terms are expressed in Eq. (32) [32]:

$$S_i = \sum_{i=1}^3 D_{ij} \mu v_j + \sum_{j=1}^3 \frac{1}{2} C_{ij} \rho |v_j| v_j \quad (32)$$

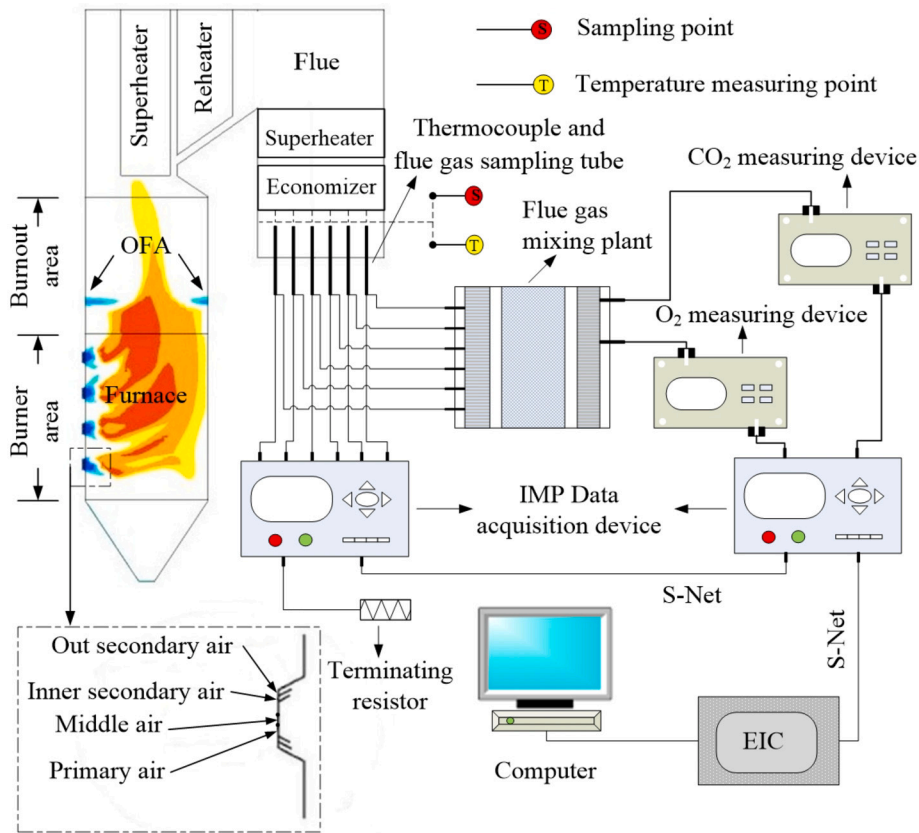


Fig. 4. Schematic diagram of test points and data acquisition system.

where, S_i is the momentum source term in direction i (x, y, z); D and C are the prescribed matrices; and v_j is the velocity component.

This simulation focused on the formation of NO_x during the combustion of pulverized coal in a furnace. Traditional post-processing methods have large errors in the prediction of NO_x distribution in the furnace. Therefore, this study uses the EDC model, which considers detailed chemical reactions during the gas phase combustion to calculate the gas phase reaction process in the furnace [33,34]. Firstly, according to the coal quality analysis, the main combustible components in the volatile matter of the pulverized coal particles were assumed to be CH₄, CO, and H₂, and the N element was assumed to exist as HCN. After the substance was released with other volatile components, as per Eq. (1), it reacted according to the NO_x model described in section 2.2.2. The coke remaining in the pulverized coal was gradually burned out, according to the particle surface reaction. The specific reactions of the particle surface reaction model are expressing using Eqs. (33)-(36) [35].



2.4. Full-scale experimental measurements

Guodian Nanjing Electric Power Test & Research Limited conducted the boiler performance assessment test after the retrofit to assess the operation indexes of the boiler unit and verify the effectiveness of the retrofit. The performance test was carried out at three loads of 135 MW, 100 MW, and 75 MW (25%) during the operation of the LNG oxygen enriched combustion system. The test content included measurements of NO_x, CO, O₂, and combustibles in the flue gas of the economizer outlet.

The measuring points were arranged on the horizontal flue at the exit of the economizer according to the multi-point grid method of equal sections, with eight holes on each side and three points per hole. The EIC data acquisition system, K-type thermocouple, T-type thermocouple, testo 350, and Fluke thermometer were used to collect and measure the composition and temperature of the flue gas point by point, as shown in Fig. 4. The flue gas analyzer was calibrated with standard gas prior to the test.

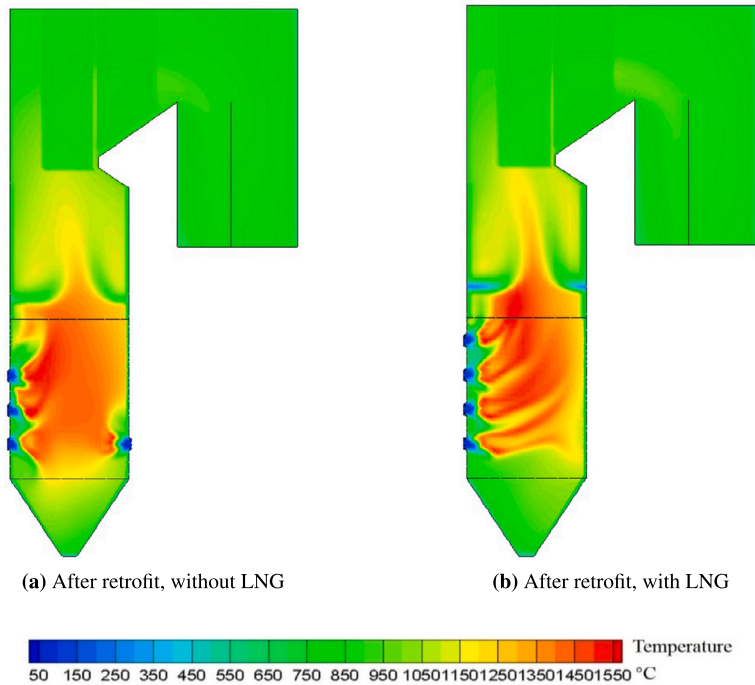


Fig. 5. The longitudinal cross-sectional temperature distribution in the furnace of Boiler No. 2 before and after the application of liquefied natural gas for 25% deep peak shaving.

3. Results and discussion

3.1. Furnace combustion characteristics under different loads

3.1.1. Combustion in the furnace

Fig. 5 shows the longitudinal section temperature distribution of the furnace of Boiler No.2 under 25% depth shaving peak conditions before and after the injection of LNG. The temperature distribution characteristics inside the furnace before and after the transformation are basically similar. In the main combustion zone, the combustion is intense, and the temperature rises sharply. It is evident that the over-fire air has sufficient rigidity to penetrate the high-temperature flames, achieving good flame suppression. Above the over-fire air, as the heat-absorbing surfaces continue to absorb heat, the flue gas temperature drops rapidly, with the average temperature at the furnace outlet being 1022 °C before the transformation and 1045 °C after. The phenomenon of flame impingement from the bottom burners was more severe before the transformation, leading to the lower part of the main combustion zone having “stacked” flames with higher temperatures. Additionally, due to the turbulent flow field near the bottom burners, some coal powder ignited prematurely, forming localized high-temperature zones near the burner exit.

Fig. 6 illustrates the distribution of high-temperature zones in the furnace under different loads. As evident high temperature areas of working conditions with load of 50% and above were relatively concentrated and distributed over a wide area, which was conducive to the stable combustion of newly injected pulverized coal. Fig. 7 shows the temperature change curve along the furnace height direction of boiler number 2 under different boiler loads. The figure indicates that the curves of the working conditions with load of 50% and above almost overlapped below 17 m, which further highlights that the modified furnace can burn stably at such loads.

Fig. 6(a) indicates that the high-temperature zone is smaller when the deep peak shaving reaches 25% load. Fig. 7 indicates that for 25% load, the maximum temperature in the furnace was lower than 1100 °C, and the overall temperature distribution in the main combustion zone was also significantly lower than the other three loads, which is not conducive to the stability of combustion and can easily extinguish fires. Therefore, this retrofit scheme opted to use an LNG enriched combustor on the second-tier combustor, and put LNG and pure oxygen into operation to stabilize combustion.

3.1.2. NO_x generation in the furnace under deep peak shaving

Fig. 8 depicts the NO concentration distribution in the longitudinal section of the furnace under various loads after the transformation. At 50% and above loads, NO was concentrated in the main combustion zone. When LNG was applied at 25% load, high NO concentration area was not noted. Further, under each load condition, reduction areas were noted, which is beneficial to NO reduction.

Fig. 9 shows the NO_x variation curve along the furnace height under different loads of furnace number 2. As evident, when the deep peak shaving reached 25%, the NO_x distribution level before and after the application of LNG was significantly reduced. The

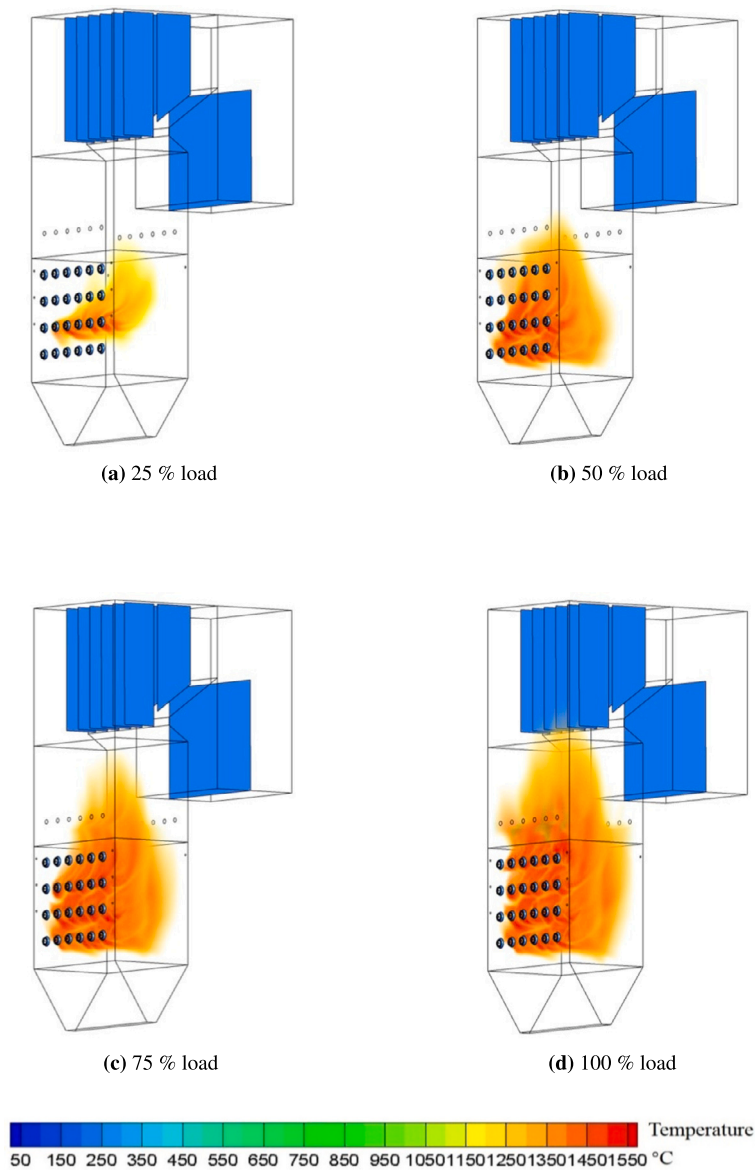


Fig. 6. Temperature distribution under different boiler loads.

NO_x emission level at the furnace outlet reduced from 380 mg/m³ to 316 mg/m³; this is lower than the retrofit requirement of 350 mg/m³.

3.1.3. Analysis of low NO_x after LNG application

In order to explore the effect of LNG on NO_x reduction, the influence of LNG under 25% load was compared and analyzed. Fig. 10 shows the NO concentration distribution in the longitudinal section of the furnace before and after LNG was applied in furnace number 2 at 25% deep peak shaving. NO_x generation with LNG was significantly reduced near the burner outlet, and the reduction zone was notably larger. When LNG was not applied, a notable amount of NO was concentrated near the combustor outlet, indicating that LNG combusted in a reducing atmosphere near the combustor outlet to generate significant number of reducing groups, which reduced the suppression of NO production.

In order to analyze the principle of steady combustion and low NO_x generation after LNG application, we followed the particle movement trajectory of the second and third burner on the front wall of the boiler into the furnace using post-processing software, as shown in Fig. 11. Next, changes in temperature and NO concentration along the process were assessed, as depicted in Fig. 12.

Fig. 12(a) indicates that after the LNG was applied, the primary air flow entered the furnace at a high temperature of ignition, and the temperature was higher than 400 °C. When the LNG was not applied, the primary air entered the furnace at a temperature of approximately 75 °C. This suggests that when LNG and pure oxygen were put into operation, active combustion was realized

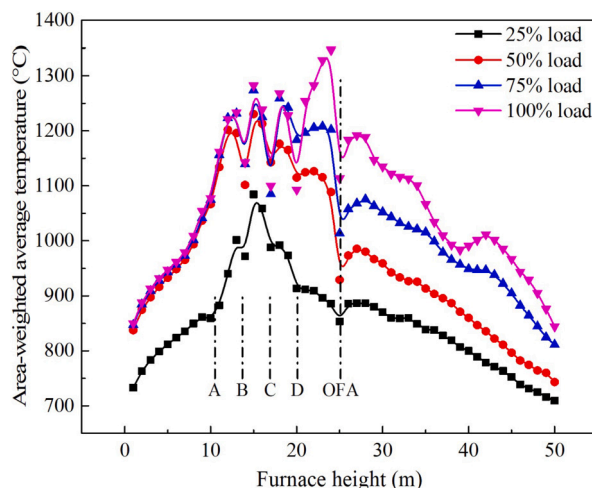


Fig. 7. Average temperature distribution profile along the furnace height.

Table 6

Measured values of NO_x, CO, and O₂ at the furnace outlet when LNG-mixed and oxygen enriched combustion system was applied after retrofit of furnace number 2.

Item	Unit	135 MW		100 MW		75 MW (25%)	
		Side A	Side B	Side A	Side B	Side A	Side B
Oxygen average value	%	3.92	3.76	1.86	2.48	5.72	5.08
		3.84		2.22		5.4	
CO average value	ppm	35.92	28.00	23.56	27.56	27.80	28.20
		31.96		25.56		28.00	
NO _x (Standard state dry basis, 6% O ₂) average value	mg/m ³	254.45	282.3	333.51	330.38	288.98	306.74
		268.38		331.95		297.86	

in the primary air duct and the combustion environment was a reducing atmosphere. Thus, the temperature of the primary air stream increased, which was conducive to the ignition and stable combustion of pulverized coal. Further, a reducing combustion environment was created, which significantly inhibited the generation of NO_x.

Fig. 12(b) shows two peak areas where NO was intensively generated when LNG was included. The first peak can be attributed to the high-temperature pulverized coal gas stream that ignited in a reducing atmosphere and released part of the HCN to generate NO, which was quickly reduced. The second peak can be attributed to the NO generated during the combustion of pulverized coal particles and was then partially reduced in the recirculation zone. In comparison, when LNG was not included, only a peak of pulverized coal combustion that quickly generated NO was noted, which was 120 ppm higher than when LNG was included; the NO was then partially reduced by the reducing groups in the reduction zone. In addition, the reduction area expanded after LNG was included, and the reduction time of NO was prolonged, which was beneficial to the further reduction of NO.

3.2. Verification of experimental measurements

Table 6 shows part of the measured data of the A side and side B of the furnace outlet under the three loads when the LNG-mixed and oxygen enriched combustion system was applied after the retrofit of boiler number 2. The results show that all the assessment values reached the retrofit target and confirm that the LNG-mixed and oxygen enriched combustion system can effectively modify the combustion performance of the boiler during deep peak shaving.

Fig. 13 compares and analyzes the experimental and calculated values of NO_x, CO, and O₂ at the furnace outlet when the LNG-mixed and oxygen enriched combustion system was put into operation at 25% load. It is evident that the model employed for this simulation, especially the NO_x model, can adapt to the combustion and NO_x prediction when the LNG-mixed and oxygen-enriched combustion system was applied. The test value error was small.

3.3. Comparison with previous research results

In the past, most of the improvement measures have been taken from the perspective of reducing the ignition and combustion characteristics of pulverized coal, and targeted retrofit measures have been proposed based on specific boiler combustion conditions, including increasing primary air temperature, raising coal concentration, and reducing primary air rate and coal fineness [36,37]. For example, Zhong Lijing et al. [38] from Guangdong Electric Power Group Zhuhai Power Plant focused on a 700 MW tangentially

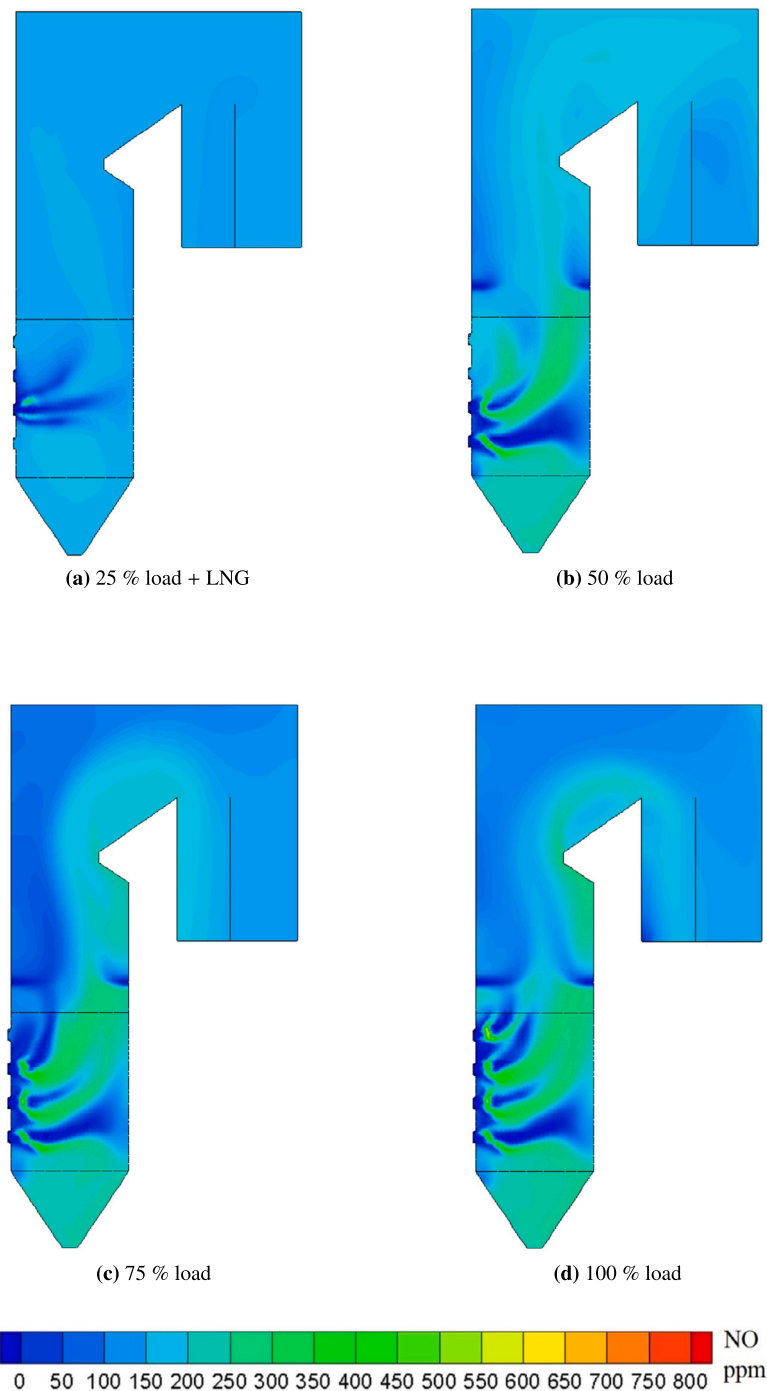


Fig. 8. NO concentration distribution in furnace longitudinal section under different loads after reformation of furnace number 2.

fired boiler, and investigated the impact of burner operation mode on boiler performance during deep-load regulation. The results indicated that when the boiler operating load is below 300 MW, the method of operating the upper three layers of burners effectively raises the reheat steam temperature, improves the turbine efficiency, and reduces the unit's coal consumption. In comparison, this paper demonstrated that after the implementation of the LNG (liquefied natural gas) rich oxygen combustion system, the primary air-coal powder gas stream actively enters the furnace in a state of active combustion. This effectively stabilizes the combustion and reduces the generation of nitrogen oxides (NO_x) by inhibiting the formation of reducing groups such as CH₃ and CH₂ from LNG, resulting in a reduction of NO_x emissions at the furnace outlet from 380 mg/m³ to 316 mg/m³, thus meeting the retrofitting objectives in a more targeted and cost-effective manner.

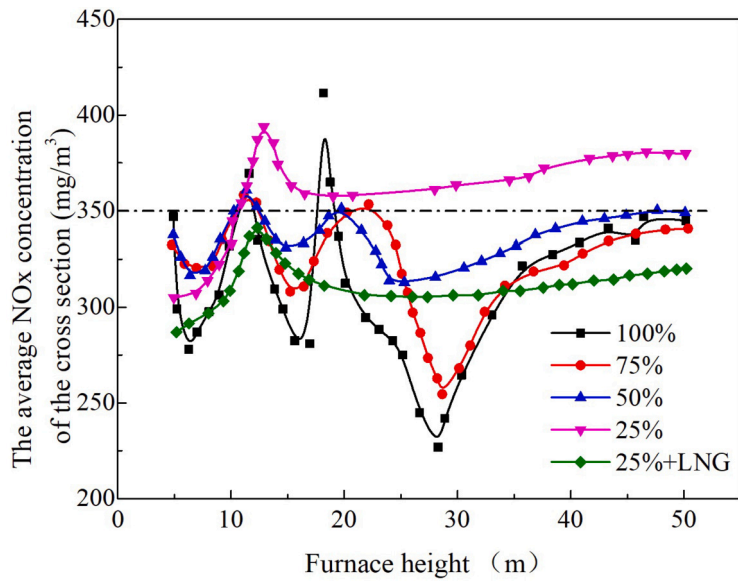


Fig. 9. NOx change curve along the furnace height under different loads in furnace number 2.

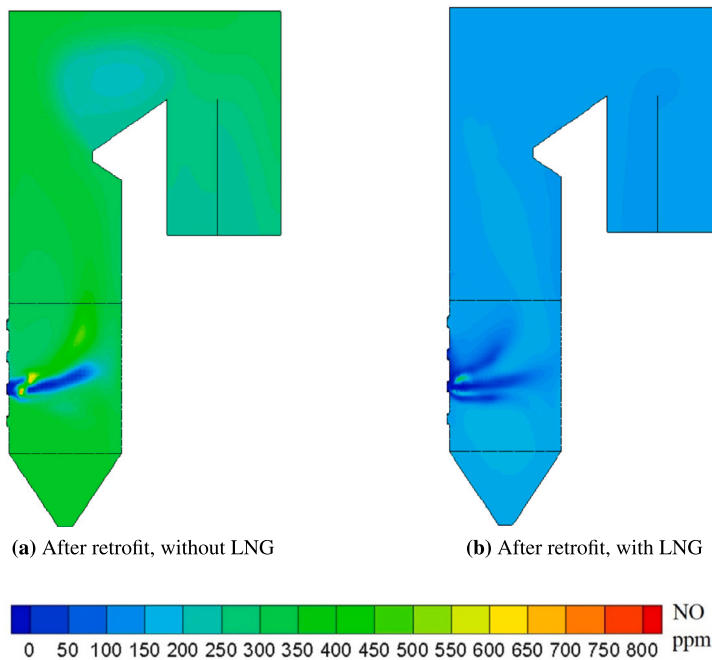


Fig. 10. NO concentration distribution in the longitudinal section of the furnace before and after LNG was applied in furnace number 2 at 25% deep peak shaving.

3.4. Economic analysis

In Boiler No. 2, only the bottom burner serves as the ignition source, while load changes are mainly adjusted by the coal air volume of other layers of burners. The layer with the ignition source ensures stable power to guarantee flame stability. When the burner approaches instability in combustion, LNG is injected. The consumption of LNG is determined by the burner and is not significantly related to the load size. It is only used at a very narrow load range, where the LNG consumption is approximately fixed at around 8.3 to 10 kilograms per hour, costing between 45 to 54 RMB per hour. The boiler is fueled with low-quality coal which is difficult to burn. Compared to the original burners using a small diesel gun for ignition with a small amount of diesel, the LNG ignition has stronger ignition capabilities. Using diesel may lead to incomplete combustion products such as soot, which can clog the electrical or bag dust removal systems. In situations of very low load, it may be impossible to resume the operation of these

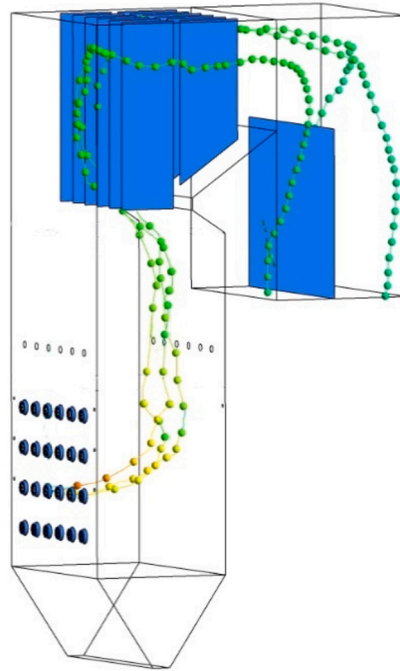


Fig. 11. Particle trajectory of the third burner on the second floor of furnace number 2.

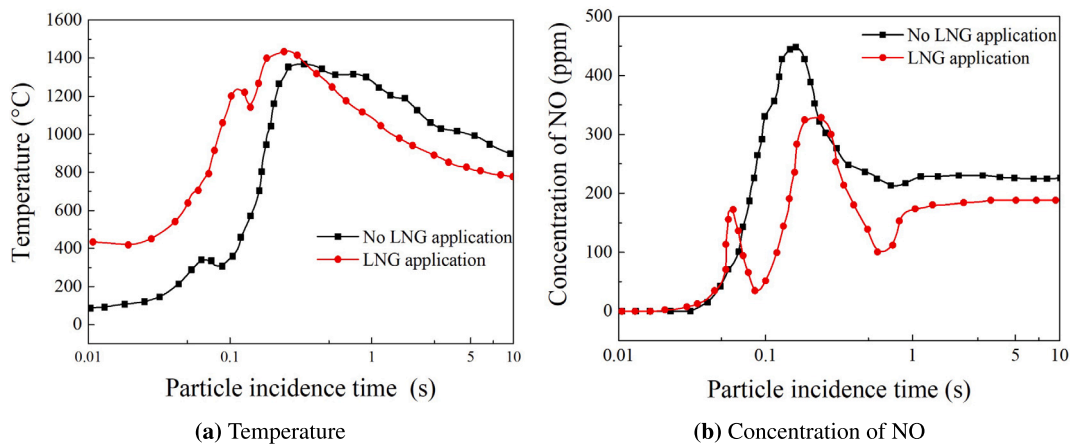


Fig. 12. Temperature and NO concentration change along the particle trajectory before and after LNG application.

dust removal devices, while using natural gas for ignition and combustion is more environmentally friendly under these low-load conditions throughout the entire process.

4. Conclusion

A retrofit scheme for deep peak shaving and low NO_x emission for a 330 MW subcritical pressure face-fired boiler located in Ningxia, China, was introduced. Chemkin software was used to construct a suitable NO_x model according to the combustion characteristics of pulverized coal blended with LNG, and a three dimensional CFD model was established. Additionally, the EDC model was used to calculate the combustion characteristics and NO_x generation in the boiler before and after the retrofit and during deep peak shaving. Some conclusions can be drawn:

(1) The proposed flexible retrofit plan of placing all four layer burners on the front wall and mixing LNG and oxygen enriched combustion in the second layer burner was successful. When the load was 50% and above, the generation of NO_x was significantly reduced; and the goal of retrofit below 350 mg/m³ was achieved. Combustion stability was also guaranteed at low load (25% BMCR), and NO_x at the furnace outlet reduced to 316 mg/m³.

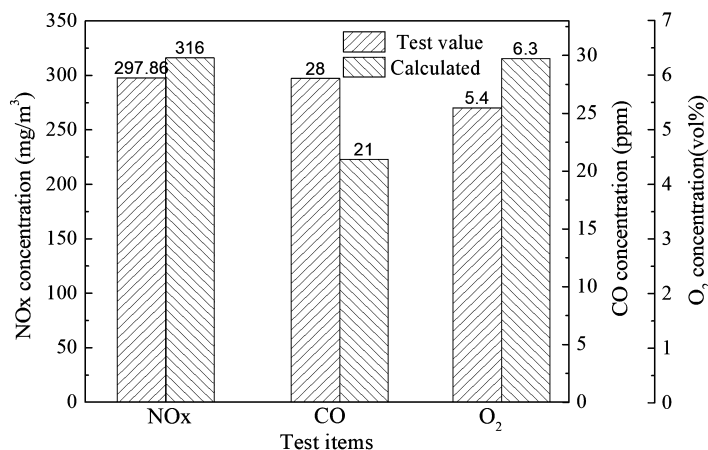


Fig. 13. Comparison of furnace outlet test value and calculated value when LNG-mixed and oxygen enriched combustion system was applied at 25% load after retrofit of furnace number 2.

(2) The NO_x model proposed in this study for co-firing pulverized coal and LNG was consistent with the test data and accurately explains the low NO_x emissions that were measured during the on-site low load test. With the help of chemical reaction kinetics, the mechanism of LNG's promotion of NO_x reduction during co-combustion was explored highlighting that a large number of reducing groups such as CH₃ and CH₂ produced by LNG inhibited NO_x production.

(3) Addition of LNG and oxygen to the center of the burner improved the stability of combustion. At 25% load, the high-temperature area of the furnace combustion was significantly reduced, and the average temperature of the furnace cross-section was lower than 1100 °C, which was not conducive to stable combustion. However, after the LNG and oxygen-fuel combustion system were operated, the primary air pulverized coal gas flow entered the furnace in a high-intensity combustion state, and the temperature in the furnace was over 400 °C, which effectively stabilized the combustion.

Data availability statement

No data was used for the research described in the article.

CRediT authorship contribution statement

Hujun Zhao: Writing – original draft, Software, Methodology, Conceptualization. **WeiQi Li:** Validation, Supervision, Software. **Jie Zhang:** Visualization, Supervision, Investigation. **Xian Ding:** Writing – review & editing, Software, Methodology, Conceptualization. **Zhizhong Kang:** Funding acquisition, Formal analysis, Data curation, Conceptualization.

Declaration of competing interest

The authors declare the following financial interests/personal relationships which may be considered as potential competing interests:

WeiQi Li reports financial support was provided by National Key Research and Development Program of China. If there are other authors, they declare that they have no known competing financial interests or personal relationships that could have appeared to influence the work reported in this paper.

Acknowledgements

This work is supported by National Key Research and Development Program of China grant number (2022YFB410-0803).

References

- [1] Y. Gu, J. Xu, D. Chen, Z. Wang, Q. Li, Overall review of peak shaving for coal-fired power units in China, *Renew. Sustain. Energy Rev.* 54 (2016) 723–731.
- [2] Q.-y. Fang, H.-c. Zhou, H.-j. Wang, Y. Bin, H.-c. Zeng, Flexibility of a 300 mw arch firing boiler burning low quality coals, *J. China Univ. Min. Technol.* 17 (4) (2007) 566–571.
- [3] Z. Lijin, D. Jian, S. Weijie, et al., Effects of burner operation mode on performance of the boiler under low load conditions, *J. Chin. Soc. Power Eng.* 35 (9) (2015) 693–698.
- [4] G. Wang, J. Deng, Y. Zhang, Q. Zhang, L. Duan, J. Hao, J. Jiang, Air pollutant emissions from coal-fired power plants in China over the past two decades, *Sci. Total Environ.* 741 (2020) 140326.
- [5] L. Ma, Q. Fang, C. Yin, H. Wang, C. Zhang, G. Chen, A novel corner-fired boiler system of improved efficiency and coal flexibility and reduced nox emissions, *Appl. Energy* 238 (2019) 453–465.

- [6] M. Kanada, L. Dong, T. Fujita, M. Fujii, T. Inoue, Y. Hirano, T. Togawa, Y. Geng, Regional disparity and cost-effective so₂ pollution control in China: a case study in 5 mega-cities, *Energy Policy* 61 (2013) 1322–1331.
- [7] W. Yang, W. Li, F. Guo, F. Yang, K. Zhang, F. Chen, Emission characteristics and controlling of nox in lean coal-fired boiler of the 330 mw, unit, *Clean Coal Technol.* 23 (2017) 107–112.
- [8] X.-B. Zhang, H. Zhao, J.-G. Yang, Study on the variation of coal properties for different coal diameters and its effects on combustion characteristics, *J. China Coal Soc.* 36 (6) (2011) 999–1003.
- [9] L. Yang, Q.L. Wen, Study of 1000 mw ultrasupercritical boiler unit oil-free minimum load stable combustion, *Power Stn. Syst. Eng.* 26 (5) (2010) 13–16.
- [10] T. Tsumura, H. Okazaki, P. Derjatin, K. Savolainen, Reducing the minimum load and nox emissions for lignite-fired boiler by applying a stable-flame concept, *Appl. Energy* 74 (3–4) (2003) 415–424.
- [11] Q. Zha, D. Li, D. Che, et al., Numerical evaluation of heat transfer and nox emissions under deep-air-staging conditions within a 600 mwe tangentially fired pulverized-coal boiler, *Appl. Therm. Eng.* 116 (2017) 170–181.
- [12] Y. Wang, Y. Zhou, N. Bai, J. Han, Experimental investigation of the characteristics of nox emissions with multiple deep air-staged combustion of lean coal, *Fuel* 280 (2020) 118416.
- [13] Z. Wang, L. Wang, P. Gao, Y. Yu, R. Wang, Analysis of composite sorbents for ammonia storage to eliminate nox emission at low temperatures, *Appl. Therm. Eng.* 128 (2018) 1382–1390.
- [14] G. Zeng, M. Xu, Y. Tu, Z. Li, Y. Cai, Z. Zheng, K. Tay, W. Yang, Influences of initial coal concentration on ignition behaviors of low-nox bias combustion technology, *Appl. Energy* 278 (2020) 115745.
- [15] R. Yoshiie, T. Kawamoto, D. Hasegawa, Y. Ueki, I. Naruse, Gas-phase reaction of nox formation in oxyfuel coal combustion at low temperature, *Energy Fuels* 25 (6) (2011) 2481–2486.
- [16] P. Glarborg, J. Miller, B. Ruscic, S. Klippenstein, *Modeling nitrogen chemistry in combustion*, 2018.
- [17] J.A. Miller, C.T. Bowman, Mechanism and modeling of nitrogen chemistry in combustion, *Prog. Energy Combust. Sci.* 15 (4) (1989) 287–338.
- [18] Q. Xiaoyang, Analysis and applications of 600 mw supercritical thermal power units without oil depth peak load regulation, *Gen. Technol.* (2015) 36–39.
- [19] S. Li, Z. Chen, E. He, B. Jiang, Z. Li, Q. Wang, Combustion characteristics and nox formation of a retrofitted low-volatile coal-fired 330 mw utility boiler under various loads with deep-air-staging, *Appl. Therm. Eng.* 110 (2017) 223–233.
- [20] S. Ti, M. Kuang, H. Wang, G. Xu, C. Niu, Y. Liu, Z. Wang, Experimental combustion characteristics and nox emissions at 50% of the full load for a 600-mwe utility boiler: effects of the coal feed rate for various Mills, *Energy* 196 (2020) 117128.
- [21] P.Z. Yonghua Li, Binxuan Zhou, Numerical simulation of low nox swirl burner retrofit, *J. Power Eng.* 34 (4) (2014).
- [22] C. Zhou, Y. Wang, Q. Jin, Q. Chen, Y. Zhou, Mechanism analysis on the pulverized coal combustion flame stability and nox emission in a swirl burner with deep air staging, *J. Energy Inst.* 92 (2) (2019) 298–310.
- [23] D. Liu, L. Yan, S. Hou, The evaluation of high temperature corrosion of the inconel 740h in simulated coal-fired environments, *Corros. Sci.* 161 (2019) 108150.
- [24] D. Merrick, Mathematical models of the thermal decomposition of coal: 1. The evolution of volatile matter, *Fuel* 62 (5) (1983) 534–539.
- [25] T. Das, Evolution characteristics of gases during pyrolysis of maceral concentrates of Russian coking coals, *Fuel* 80 (4) (2001) 489–500.
- [26] Z. Li, Z. Miao, X. Shen, J. Li, Prevention of boiler performance degradation under large primary air ratio scenario in a 660 mw brown coal boiler, *Energy* 155 (2018) 474–483.
- [27] A. Silaen, T. Wang, Effect of turbulence and devolatilization models on coal gasification simulation in an entrained-flow gasifier, *Int. J. Heat Mass Transf.* 53 (9–10) (2010) 2074–2091.
- [28] M. Agraniotis, N. Nikolopoulos, A. Nikolopoulos, P. Grammelis, E. Kakaras, Numerical investigation of solid recovered fuels' co-firing with brown coal in large scale boilers—evaluation of different co-combustion modes, *Fuel* 89 (12) (2010) 3693–3709.
- [29] H. Kobayashi, J. Howard, A.F. Sarofim, Coal devolatilization at high temperatures, *Symp., Int., Combust.* 16 (1) (1977) 411–425.
- [30] A. Bestman, Two-dimensional fluctuating flow and heat transfer to a relativistic radiating gas, *Astrophys. Space Sci.* 186 (1991) 1–6.
- [31] P.D. Nguyen, G. Ghazal, V.C. Piñera, V. Battaglia, A. Rensgard, T. Ekman, M. Gazdallah, Modelling of flameless oxy-fuel combustion with emphasis on radiative heat transfer for low calorific value blast furnace gas, *Energy Proc.* 120 (2017) 492–499.
- [32] C. Xing-Xing, J. Bao-Sheng, Z. Wen-Qi, Numerical simulation of additionally installed scr denitrification equipment, *Therm. Power Gener.* 38 (2009) 51–54.
- [33] M. Rehm, P. Seifert, B. Meyer, Theoretical and numerical investigation on the edc-model for turbulence–chemistry interaction at gasification conditions, *Comput. Chem. Eng.* 33 (2) (2009) 402–407.
- [34] C. Kai, L. Bing, W. Yuxin, Y. Hairui, L. Junfu, H. Zhang, Numerical simulation of oxy-coal combustion for a swirl burner with edc model, *Chin. J. Chem. Eng.* 22 (2) (2014) 193–201.
- [35] Z. Wang, Y. Deguchi, T. Kamimoto, K. Tainaka, K. Tanno, Pulverized coal combustion application of laser-based temperature sensing system using computed tomography–tunable diode laser absorption spectroscopy (ct-tdlas), *Fuel* 268 (2020) 117370.
- [36] X. Qin, Analysis and application of deep load adjustment technology without oil injection for a 600 mw supercritical thermal power unit, *Chin. Power Ind.* (2015) (Technical Edition).
- [37] M. Richter, F. Mollenbruck, F. Obermuller, A. Knaut, F. Weiser, H. Lens, D. Lehmann, Flexibilization of steam power plants as partners for renewable energy systems, in: *Power System Computation Conference*, 2016.
- [38] L. Zhong, J. Zhong, W. Sun, L. Yuan, Q. Fang, P. Tan, The operating mode of the burner under low load in English has an impact on the boiler performance, *J. Power Eng.* 35 (9) (2015) 6.